

Two years of *Ulysses* dust data

E. Grün,¹ M. Baguhl,¹ N. Divine,² H. Fechtig,¹ D. P. Hamilton,¹ M. S. Hanner,² J. Kissel,¹ B.-A. Lindblad,³
D. Linkert,¹ G. Linkert,¹ I. Mann,⁴ J. A. M. McDonnell,⁵ G. E. Morfill,⁶ C. Polansky,² R. Riemann,¹
G. Schwehm,⁷ N. Siddique,¹ P. Staubach¹ and H. A. Zook⁸

¹Max-Planck-Institut für Kernphysik, 69029 Heidelberg, Germany

²Jet Propulsion Laboratory, Pasadena, CA 91109, U.S.A.

³Lund Observatory, 221 Lund, Sweden

⁴Max-Planck-Institut für Aeronomie, 37191 Katlenburg-Lindau, Germany

⁵University of Kent, Canterbury CT2 7NR, U.K.

⁶Max-Planck-Institut für Extraterrestrische Physik, 85748 Garching, Germany

⁷ESTEC, 2200 AG Noordwijk, The Netherlands

⁸NASA Johnson Space Center, Houston, TX 77058, U.S.A.

Received 14 September 1994; accepted 7 December 1994

Abstract. From October 18, 1990 to February 8, 1992 the *Ulysses* spacecraft traversed interplanetary space between the Earth and Jupiter; at Jupiter the spacecraft was deflected below the ecliptic onto a highly-inclined orbit ($i \sim 80^\circ$). Here, we report on dust impact data obtained from launch until the end of 1992, nearly a year after the Jupiter flyby. During that time (792 days), the *Ulysses* dust detector recorded 968 impacts of dust particles with masses ranging from 10^{-16} g to 10^{-8} g. The impact rate varied from as low as one impact per week during quiet times to more than one per minute during the dust stream of March 10–11, 1992. In this paper, we present and describe the complete data set including both raw and reduced data. The performance of the sensor, which has been very satisfactory so far, is discussed in detail together with the noise discrimination scheme employed. The instrument's detection threshold is given as a function of both the particle's mass and its speed relative to *Ulysses*. The derived impact rates and the distribution of particle masses, speeds and impact directions are compared to a model of the meteoroid complex.

Introduction

The *Ulysses* Dust Detector, and its twin instrument the *Galileo* Dust Detector, are highly sensitive multi-coincidence impact ionization sensors. The instruments have been described previously by Grün *et al.* (1992a, b) and a

detailed description of their sensitivities is presented in a companion paper (Grün *et al.*, 1995a; henceforth Paper I). Data from the *Ulysses* dust experiment have been published during all stages of the mission. Initial measurements and instrument performance were presented by Grün *et al.* (1992c, d) and Baguhl *et al.* (1992). Measurements obtained during the Jupiter flyby are described by Grün *et al.* (1992e). The discoveries of jovian dust streams and interstellar dust are discussed by Grün *et al.* (1993). Detailed re-analysis of the full data set by Baguhl *et al.* (1993) has revealed "small" impacts that were previously ignored.

Other relevant papers consider flybys of comets or asteroids (Riemann and Grün, 1992; Hamilton and Burns, 1992). Implications of *Ulysses* data with respect to zodiacal light and other interplanetary meteoroid measurements have been discussed by Mann *et al.* (1992), Divine (1993), and Mann and Grün (1993). Further analyses of the jovian streams detected with the *Ulysses* dust detector can be found in Horanyi *et al.* (1993a, b), and in Hamilton and Burns (1993). Aspects of interstellar dust detection are discussed by Grün *et al.* (1994) and Baguhl *et al.* (1994).

The purpose of this paper is to present both raw and reduced dust data obtained by *Ulysses* from October 1990 to the end of 1992 for further analysis by researchers external to the *Galileo* and *Ulysses* Dust Science Team. The main data product is a table of all impacts (both raw and reduced data) received on the ground. Together with papers on the reduction of *Galileo* and *Ulysses* dust data (Paper I) and on the first three years of *Galileo* dust data (Grün *et al.*, 1995b, Paper II), this set represents a detailed account of dust measurements from the initial phases of

the *Galileo* and *Ulysses* missions. The information presented in the three papers is equivalent to data which we are submitting to the various data archiving centers (Planetary Data System, NSSDC, *Ulysses* Data Center, etc.).

Mission and instrument operations

The purpose of the *Ulysses* mission is to explore the solar system within a few astronomical units (1–5.4 AU) of the Sun over a wide range of ecliptic latitudes (-80 to $+80^\circ$). After launch in October 1990 *Ulysses* flew on a direct trajectory to Jupiter where it was deflected onto its out-of-ecliptic orbit (Fig. 1). Table 1 gives a set of orbital elements suitable for approximating the different portions of the trajectory. By the end of 1992, *Ulysses* had reached an ecliptic latitude of -15.6° . The spacecraft is spinning with its spin axis pointing within a few degrees of the Earth; Fig. 2 plots the deviation of the spin axis from the Earth direction during the period considered. More details of the *Ulysses* mission and spacecraft itself can be found in Wenzel *et al.* (1992).

The *Ulysses* mission provides continuous data coverage for all of its instruments. Each data record containing the full information about a single dust impact consists of 128 bits of data. During the maximum real-time data transmission rate of 1024 bits s^{-1} , dust data are transmitted at 8 bits s^{-1} . Nominally this occurs for 8 h per day; during the remaining 16 h, data from all instruments are recorded on board at half the nominal rate and are transmitted to ground along with the next real-time transmission. Sometimes, due to radio link limitations, the data transmission or recording rate dropped to as low as 128 bits s^{-1} and the dust data rate dropped correspondingly.

Significant mission and dust instrument events are listed in Table 2. The dust instrument was switched on three weeks after launch at which point dust measurements commenced. During occasional in-flight noise tests, the instrument was put into a highly sensitive state so that the

noise behavior could be measured. During most of the time, however, it was kept at a state where only about ten clearly identifiable noise events occurred per day.

During the initial mission phase, the interior of the sensor was illuminated by the Sun which heated it significantly. Because of the noise produced by photoelectrons the channeltron high voltage, which determines the sensitivity of the instrument, was only gradually increased to $HV = 3$ (1137 V). The nominal high voltage $HV = 4$ (1250 V) could not be reached because of unexpected noise on the channeltron. The *Galileo* detector experienced the same noise, and it is assumed that the nearby radioactive thermal generators (RTGs) are to blame although other causes cannot be excluded. During ground tests (without RTGs) no such noise was observed.

Strong noise was also observed during sounder operation of the URAP experiment (Stone *et al.*, 1992) aboard *Ulysses*. This interference, which was not expected, caused significant dead time (about 20%) for the dust instrument. After reducing the sounder operation to a lower rate, acceptable dead times of a few percent were achieved. Other noise sources identified during the mission include direct sunlight into the dust sensor as well as energetic particles from solar flares or radiation belts (Baguhl *et al.*, 1992, 1993). Despite the high noise rates during these times, true dust impacts can still be identified. As an example, in Fig. 3 we show details of the impact and noise rates during the Jupiter flyby.

The only anomaly detected in the instrument performance was that for about 20% of all events the sector counter (SEC) did not give the correct value; instead subsequent events inherited the previous SEC value. This effect was traced to a timing error in the instrument electronics and through reprogramming of the *Ulysses* instrument in 1993, the flaw was corrected.

Impact events

During the initial 26 months of the *Ulysses* mission, complete data corresponding to 15,747 events including 968

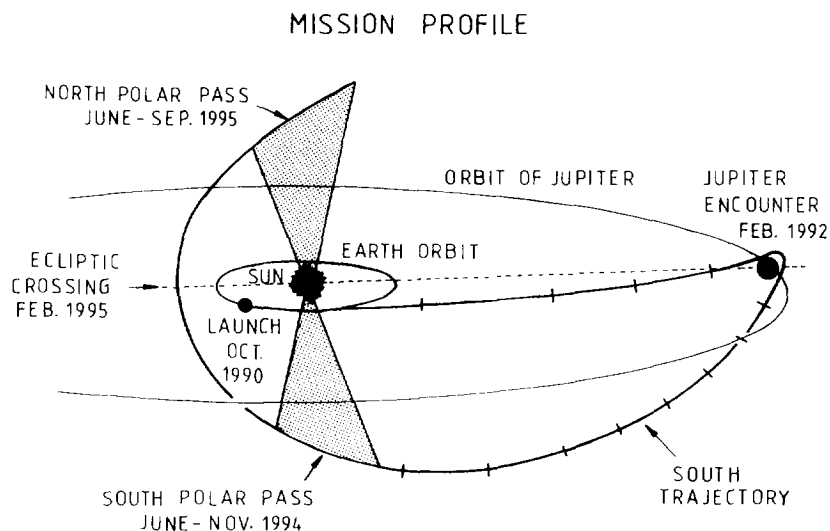


Fig. 1. A depiction of the *Ulysses* orbit showing the three major stages of the mission: the in-ecliptic trajectory to Jupiter, the Jupiter encounter and the highly inclined pass over the solar poles. The tick marks along the orbit are spaced 100 days apart. Dust data given in this paper covers the *Ulysses* orbit from launch to about the third tick mark after Jupiter

Table 1. Three sets of orbital elements that approximate different parts of the *Ulysses* trajectory—the in-ecliptic leg, the Jupiter flyby, and the out-of-ecliptic leg (AU = 149, 597, 871 km, $R_J = 71,398$ km)

| Orbital elements | | Valid time range (error < 300,000 km) |
|-------------------------------------|---------------------------|--|
| <i>In-ecliptic orbit branch</i> | | |
| Epoch | 1991 Jul. 18 21 : 00 : 54 | |
| Perihelion | 0.99546 AU | |
| Eccentricity | 0.89001 | 1990–286 12 : 00 |
| Inclination | 1.9926 | to |
| Long. of asc. node | 12.688 | 1991–341 12 : 00 |
| Arg. of perihelion | 7.9595 | |
| Mean anomaly | 10.105 | |
| True anomaly | 123.10 | |
| <i>Jovicentric orbit</i> | | |
| Epoch | 1992 Feb. 08 12 : 01 : 10 | |
| Perijove | 6.3050 R_J | |
| Eccentricity | 1.6625 | 1991–341 12 : 00 |
| Inclination | 142.23 | to |
| Long. of asc. node | 316.95 | 1992–145 00 : 00 |
| Arg. of perihelion | 127.70 | |
| Mean anomaly | 0.0099 | |
| <i>Out-of-ecliptic orbit branch</i> | | |
| Epoch | 1992 Dec. 30 21 : 00 : 04 | |
| Perihelion | 1.3408 AU | |
| Eccentricity | 0.60238 | 1992–145 00 : 00 |
| Inclination | 79.184 | to |
| Long. of asc. node | 337.51 | 1993–001 00 : 00 |
| Arg. of perihelion | 358.88 | |
| Mean anomaly | 232.33 | |
| True anomaly | 196.98 | |

dust impacts were received on the ground. Table 3 displays the number of dust impacts detected in intervals of about 7 days. Many of the noise events were recorded during the rare times when both the sounder was operating and

the dust instrument was configured to its high sensitive state for noise tests. At these times, 14 noise events were recorded in three high amplitude categories: seven events in AC21, two in AC31 and five in AC12. Here “ACxy”

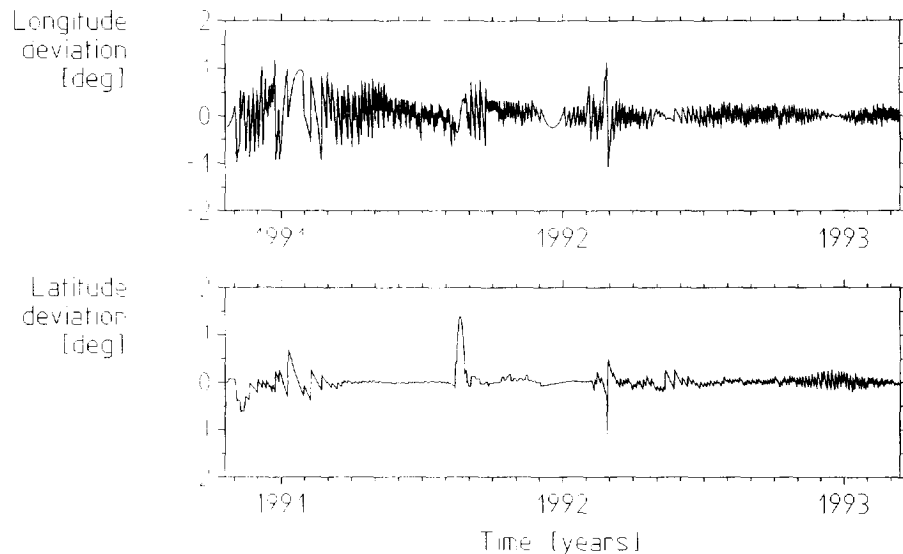


Fig. 2. The deviation of the spin axis orientation from the nominal Earth-pointing alignment both in longitude and latitude. Both angles are given in the coordinate system referred to the 1950.0 Earth mean ecliptic and equinox

Table 2. *Ulysses* mission and dust detector (DUST) configurations, tests, and other events

| Yr-DOY | Date | Time | Event |
|--------|----------------|-------|--|
| 90-279 | (6 Oct. 1990) | | <i>Ulysses</i> launch |
| 90-292 | (19 Oct. 1990) | | DUST cover release |
| 90-300 | (27 Oct. 1990) | 18:52 | DUST on, test and configuration: HV = 0, EVD = C, I, E; SSEN = 0, 0, 0, 0, short time |
| 90-301 | (28 Oct. 1990) | 00:13 | DUST configuration: EVD = I, SSEN = 0, 0, 1, 1 |
| 90-303 | (30 Oct. 1990) | 18:04 | DUST noise test, counter reset |
| 90-304 | (31 Oct. 1990) | 18:09 | DUST noise test |
| 90-305 | (1 Nov. 1990) | 18:23 | DUST noise test |
| 90-308 | (4 Nov. 1990) | 07:00 | DUST begin of sounder interferences |
| 90-310 | (6 Nov. 1990) | 19:32 | DUST noise test, configuration: HV = 1, EVD = C, I |
| 90-311 | (7 Nov. 1990) | 17:45 | DUST noise test, sounder interference test |
| 90-319 | (15 Nov. 1990) | 19:30 | DUST reduced sounder interference |
| 90-324 | (20 Nov. 1990) | 19:30 | DUST noise test, sounder interference test |
| 90-344 | (10 Dec. 1990) | 17:54 | DUST noise test, sounder interference test, configuration: HV = 2 |
| 90-354 | (20 Dec. 1990) | 19:22 | DUST noise test, sounder interference test |
| 91-002 | (2 Jan. 1991) | 18:48 | DUST noise test, configuration: HV = 3, EVD = C, I, E; SSEN = 0, 0, 0, 1 |
| 91-014 | (14 Jan. 1991) | 21:44 | DUST configuration: EVD = C, I |
| 91-037 | (6 Feb. 1991) | 00:50 | DUST configuration: HV = 1 |
| 91-165 | (14 June 1991) | 15:04 | <i>Ulysses</i> anomaly, DUST off |
| 91-169 | (18 June 1991) | 17:00 | DUST on, configuration: HV = 1, EVD = C, I, SSEN = 0, 0, 0, 1 |
| 91-297 | (24 Oct. 1991) | 14:16 | DUST noise test |
| 91-330 | (26 Nov. 1991) | 16:00 | DUST configuration: HV = 3 |
| 92-034 | (3 Feb. 1992) | 00:10 | DUST configuration: HV = 2 |
| 92-038 | (7 Feb. 1992) | 18:18 | DUST configuration: HV = 1, EVD = I, SSEN = 1, 0, 0, 1 |
| 92-038 | (7 Feb. 1992) | 19:18 | DUST configuration: SSEN = 2, 0, 2, 2 |
| 92-038 | (7 Feb. 1992) | 20:18 | DUST configuration: SSEN = 3, 1, 3, 3 |
| 92-039 | (8 Feb. 1992) | 12:04 | <i>Ulysses</i> Jupiter closest approach |
| 92-040 | (9 Feb. 1992) | 02:21 | DUST configuration: SSEN = 2, 0, 2, 2 |
| 92-040 | (9 Feb. 1992) | 03:21 | DUST configuration: SSEN = 1, 0, 1, 1 |
| 92-040 | (9 Feb. 1992) | 04:21 | DUST configuration: HV = 2, EVD = C, I, SSEN = 0, 0, 0, 1 |
| 92-041 | (10 Feb. 1992) | 17:00 | DUST configuration: HV = 3 |
| 92-320 | (15 Nov. 1992) | 11:50 | DUST noise test |

Abbreviations used to describe the instrument configuration: HV, channeltron high voltage step; EVD, event definition, ion- (I), channeltron- (C), or electron-channel (E); SSEN, detection thresholds ICP, CCP, ECP, and PCP.

refers to class number “x” and amplitude range “y” (for a detailed description of the accumulator categories see Paper I).

During these and other noisy periods (noise tests, initial

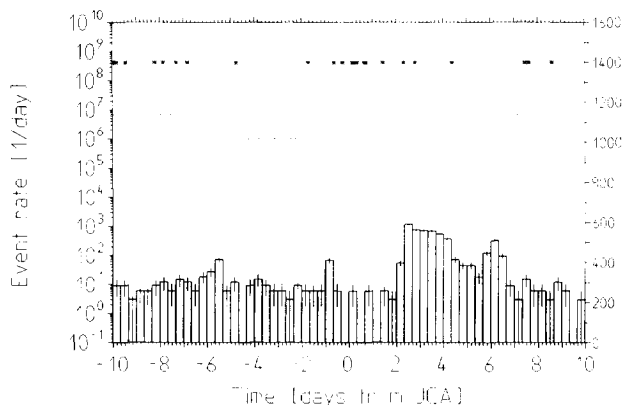


Fig. 3. Details of the measurements during Jupiter flyby. The bars in the lower part of the figure and the left scale indicate the noise rate. The voltage on the channeltron is indicated by the dotted line and the right scale; its value was lowered by ground command during the flyby to reduce noise events. Finally, dust impacts are indicated by stars in the upper part of the figure

sounder operations, solar flare events or radiation belt crossings) many events were recorded only as “counts” since their charge amplitudes and other characteristics were overwritten before the data could be transmitted to ground (see bottom of Table 3). Since the dust impact rate was low during times surrounding these periods, it is expected that no true dust impacts were lost. Only during the main dust stream on March 10 and 11, 1992, when impact rates were extremely high, were complete data from some true impacts not recorded. Approximately 190 additional stream particle impacts (Baguhl, 1993) were only counted and have to be added to the 369 stream particles for which full information was recovered. The missing stream particles all belong to the AC01, AC11 and AC02 categories. With the exception of these three categories and a single particle in the AC23 category, complete information of all true dust impacts was successfully transmitted to Earth.

A list of all 968 impacts completely received on the ground is displayed in Table 4. Dust particles are identified by a sequence number and their impact time. The event category—class (CLN) and amplitude range (AR)—are also given. Raw data as received on ground are displayed next: sector value (SEC) at time of impact, impact charge

Table 3. (*Continued*)

| Date | Time | r(AU) | Δt (d) | AC 01 | AC 11 | AC 21 | AC 31 | AC 02 | AC 12 | AC 22 | AC 32 | AC 03 | AC 13 | AC 23 | AC 33 | AC 04 | AC 14 | AC 24 | AC 34 | AC 05 | AC 15 | AC 25 | AC 35 | AC 06 | AC 16 | AC 26 | AC 36 | |
|----------------------------|-------|-------|----------------|-------|-------|-------|-------|-------|-------|-------|-------|-------|-------|-------|-------|-------|-------|-------|-------|-------|-------|-------|-------|-------|-------|-------|-------|---|
| 92/010 | 00:01 | 5.159 | 7.0 | * | * | - | 5 | * | 1 | - | - | - | - | - | - | - | - | - | - | - | - | - | - | - | - | - | - | - |
| 92/017 | 00:03 | 5.215 | 7.0 | * | * | - | 2 | * | - | - | 1 | - | - | - | - | - | - | - | - | - | - | - | - | - | - | - | - | - |
| 92/024 | 00:00 | 5.269 | 7.0 | * | * | - | 2 | * | 1 | - | - | - | - | - | - | - | - | - | - | - | - | - | - | - | - | - | - | - |
| 92/031 | 00:03 | 5.326 | 7.0 | * | * | - | - | * | 1 | - | - | - | - | - | - | - | - | - | - | - | - | - | - | - | - | - | - | - |
| 92/038 | 00:02 | 5.385 | 7.0 | * | * | - | - | * | - | - | - | - | - | - | - | - | - | - | - | - | - | - | - | - | - | - | - | - |
| 92/040 | 00:02 | 5.402 | 2.0 | * | * | - | - | * | 1 | - | - | - | - | - | - | - | - | - | - | - | - | - | - | - | - | - | - | - |
| 92/042 | 00:02 | 5.403 | 2.0 | * | * | - | - | * | 2 | - | - | - | - | - | - | - | - | - | - | - | - | - | - | - | - | - | - | - |
| 92/049 | 00:00 | 5.403 | 7.0 | * | * | - | - | * | - | - | 1 | - | - | - | - | - | - | - | - | - | - | - | - | - | - | - | - | - |
| 92/056 | 00:04 | 5.402 | 7.0 | * | * | - | 1 | * | 1 | - | - | - | - | - | - | - | - | - | - | - | - | - | - | - | - | - | - | - |
| 92/070 | 00:00 | 5.400 | 14.0 | * | * | - | - | * | 1 | - | - | - | - | - | - | - | - | - | - | - | - | - | - | - | - | - | - | - |
| 92/077 | 00:01 | 5.398 | 7.0 | * | * | - | 110 | * | 1 | - | - | - | - | - | - | - | - | - | - | - | - | - | - | - | - | - | - | - |
| 92/084 | 00:00 | 5.397 | 7.0 | * | * | - | - | * | - | - | - | - | - | - | - | - | - | - | - | - | - | - | - | - | - | - | - | - |
| 92/092 | 00:03 | 5.394 | 8.0 | * | * | - | - | * | - | - | 1 | - | - | - | - | - | - | - | - | - | - | - | - | - | - | - | - | - |
| 92/099 | 00:03 | 5.392 | 7.0 | * | * | - | 4 | * | - | - | - | - | - | - | - | - | - | - | - | - | - | - | - | - | - | - | - | - |
| 92/106 | 00:05 | 5.389 | 7.0 | * | * | - | 5 | * | - | - | - | - | - | - | - | - | - | - | - | - | - | - | - | - | - | - | - | - |
| 92/113 | 00:01 | 5.386 | 7.0 | * | * | - | 2 | * | - | - | 1 | - | - | - | - | - | - | - | - | - | - | - | - | - | - | - | - | - |
| 92/127 | 00:02 | 5.379 | 14.0 | * | * | - | 6 | * | - | - | 2 | - | - | - | - | - | - | - | - | - | - | - | - | - | - | - | - | - |
| 92/134 | 00:00 | 5.375 | 7.0 | * | * | - | - | * | - | - | 1 | - | - | - | - | - | - | - | - | - | - | - | - | - | - | - | - | - |
| 92/141 | 00:00 | 5.370 | 7.0 | * | * | - | - | * | 1 | - | - | - | - | - | - | - | - | - | - | - | - | - | - | - | - | - | - | - |
| 92/148 | 00:04 | 5.366 | 7.0 | * | * | - | - | * | 1 | - | - | - | - | - | - | - | - | - | - | - | - | - | - | - | - | - | - | - |
| 92/155 | 00:03 | 5.361 | 7.0 | * | * | - | - | * | 1 | - | - | - | - | - | - | - | - | - | - | - | - | - | - | - | - | - | - | - |
| 92/162 | 00:00 | 5.356 | 7.0 | * | * | - | 4 | * | - | - | - | - | - | - | - | - | - | - | - | - | - | - | - | - | - | - | - | - |
| 92/169 | 00:00 | 5.350 | 7.0 | * | * | - | - | * | - | - | 1 | - | - | - | - | - | - | - | - | - | - | - | - | - | - | - | - | - |
| 92/176 | 00:03 | 5.344 | 7.0 | * | * | - | - | * | - | - | 1 | - | - | - | - | - | - | - | - | - | - | - | - | - | - | - | - | - |
| 92/190 | 00:00 | 5.332 | 14.0 | * | * | - | 2 | * | - | - | - | - | - | - | - | - | - | - | - | - | - | - | - | - | - | - | - | - |
| 92/204 | 00:07 | 5.318 | 14.0 | * | * | - | - | * | - | - | - | - | - | - | - | - | - | - | - | - | - | - | - | - | - | - | - | - |
| 92/225 | 00:00 | 5.295 | 21.0 | * | * | - | - | * | 1 | - | - | - | - | - | - | - | - | - | - | - | - | - | - | - | - | - | - | - |
| 92/232 | 00:03 | 5.287 | 7.0 | * | * | - | - | * | - | - | - | - | - | - | - | - | - | - | - | - | - | - | - | - | - | - | - | - |
| 92/246 | 00:02 | 5.270 | 14.0 | * | * | - | 1 | * | - | - | - | - | - | - | - | - | - | - | - | - | - | - | - | - | - | - | - | - |
| 92/253 | 00:00 | 5.260 | 7.0 | * | * | - | 1 | * | - | - | 1 | - | - | - | - | - | - | - | - | - | - | - | - | - | - | - | - | - |
| 92/260 | 00:00 | 5.251 | 7.0 | * | * | - | - | * | - | - | - | - | - | - | - | - | - | - | - | - | - | - | - | - | - | - | - | - |
| 92/267 | 00:02 | 5.241 | 7.0 | * | * | - | - | * | 1 | - | - | - | - | - | - | - | - | - | - | - | - | - | - | - | - | - | - | - |
| 92/288 | 00:05 | 5.210 | 21.0 | * | * | - | - | * | - | - | - | - | - | - | - | - | - | - | - | - | - | - | - | - | - | - | - | - |
| 92/295 | 00:05 | 5.199 | 7.0 | * | * | - | 1 | * | 1 | - | - | - | - | - | - | - | - | - | - | - | - | - | - | - | - | - | - | - |
| 92/302 | 00:05 | 5.187 | 7.0 | * | * | - | 2 | * | 1 | - | - | - | - | - | - | - | - | - | - | - | - | - | - | - | - | - | - | - |
| 92/309 | 00:05 | 5.176 | 7.0 | * | * | - | - | * | - | - | 1 | - | - | - | - | - | - | - | - | - | - | - | - | - | - | - | - | - |
| 92/316 | 00:00 | 5.164 | 7.0 | * | * | - | - | * | - | - | 1 | - | - | - | - | - | - | - | - | - | - | - | - | - | - | - | - | - |
| 92/323 | 00:08 | 5.151 | 7.0 | * | * | - | - | * | 1 | - | - | - | - | - | - | - | - | - | - | - | - | - | - | - | - | - | - | - |
| 92/330 | 00:08 | 5.139 | 7.0 | * | * | - | - | * | - | - | 2 | - | - | - | - | - | - | - | - | - | - | - | - | - | - | - | - | - |
| 92/337 | 00:01 | 5.126 | 7.0 | * | * | - | - | * | - | - | - | - | - | - | - | - | - | - | - | - | - | - | - | - | - | - | - | - |
| 92/344 | 00:02 | 5.113 | 7.0 | * | * | - | - | * | - | - | 1 | - | - | - | - | - | - | - | - | - | - | - | - | - | - | - | - | - |
| 92/351 | 00:02 | 5.099 | 7.0 | * | * | - | - | * | - | - | - | - | - | - | - | - | - | - | - | - | - | - | - | - | - | - | - | - |
| 92/358 | 00:00 | 5.085 | 7.0 | * | * | - | 1 | * | - | - | 1 | - | - | - | - | - | - | - | - | - | - | - | - | - | - | - | - | - |
| 92/365 | 00:06 | 5.071 | 7.0 | * | * | - | - | * | - | - | 2 | - | - | - | - | - | - | - | - | - | - | - | - | - | - | - | - | - |
| Impacts (counted) | | | | * | * | 0 | 163 | * | 32 | 2 | 66 | 3 | 9 | 2 | 42 | 0 | 0 | 0 | 12 | 0 | 0 | 0 | 1 | 0 | 1 | 0 | 1 | 1 |
| Impacts (complete data) | | | | 555 | 37 | 0 | 163 | 43 | 32 | 2 | 66 | 3 | 9 | 1 | 42 | 0 | 0 | 0 | 12 | 0 | 0 | 0 | 1 | 0 | 1 | 0 | 1 | 1 |
| All events (complete data) | | | | 13093 | 2060 | 7 | 165 | 245 | 37 | 2 | 66 | 5 | 9 | 1 | 42 | 0 | 0 | 0 | 12 | 0 | 0 | 0 | 1 | 0 | 1 | 0 | 1 | 1 |

Table 4. Raw data : No., impact time, CLN, AR, SEC, IA, EA, CA, IT, ET, EIT, EIC, IIC, PA, PET, EVD, ICP, ECP, CCP, PCP, HV ; and evaluated data : R, LON, LAT, D_{imp} , rotation angle (ROT), instr. pointing (S_{LON} , S_{LAT}), speed (v), speed error factor (VEF), mass (m) and mass error factor (MEF)

| No. | IMP. DATE | C | AR | S | IA | EA | CA | IT | ET | E | I | PA | R | LON | LAT | D_{imp} | ROT | S_{LON} | S_{LAT} | V | VEF | M | MEF |
|-----|--------------|---|----|-----|----|----|----|----|----|----|---|----|----|---------|------|-----------|---------|-----------|-----------|-----|------|------|-------------------------|
| 1 | 90-301 13:51 | 0 | 1 | 200 | 5 | 12 | 0 | 6 | 7 | 7 | 0 | 35 | 0 | 1.02835 | 41.8 | 1.0 | 10806.8 | 171 | 191 | -80 | 43.5 | 1.9 | 2.4 · 10 ⁻¹⁵ |
| 2 | 90-301 18:46 | 0 | 1 | 149 | 2 | 13 | 0 | 15 | 14 | 0 | 1 | 0 | 0 | 1.02937 | 42.1 | 1.0 | 10795.8 | 99 | 207 | -9 | 11.8 | 11.8 | 1.7 · 10 ⁻¹³ |
| 3 | 90-302 03:12 | 0 | 3 | 173 | 23 | 28 | 0 | 13 | 6 | 0 | 0 | 31 | 1 | 1.03092 | 42.6 | 1.0 | 10779.2 | 133 | 204 | -42 | 8.6 | 5.2 | 6.9 · 10 ⁻¹¹ |
| 4 | 90-302 21:34 | 0 | 1 | 158 | 2 | 8 | 0 | 15 | 7 | 6 | 0 | 0 | 1 | 1.03412 | 43.6 | 1.0 | 10746.0 | 112 | 206 | -21 | 56.0 | 2.0 | 2.6 · 10 ⁻¹⁶ |
| 5 | 90-302 22:04 | 0 | 1 | 161 | 3 | 10 | 0 | 8 | 7 | 8 | 0 | 0 | 1 | 1.03412 | 43.6 | 1.0 | 10746.0 | 116 | 205 | -25 | 21.4 | 1.9 | 1.7 · 10 ⁻¹⁴ |
| 6 | 90-303 04:24 | 0 | 1 | 130 | 2 | 7 | 0 | 8 | 7 | 6 | 0 | 0 | 1 | 1.03521 | 43.9 | 1.0 | 10734.9 | 72 | 211 | 17 | 36.7 | 2.0 | 1.3 · 10 ⁻¹⁵ |
| 7 | 90-303 13:09 | 0 | 2 | 46 | 9 | 14 | 0 | 7 | 5 | 0 | 0 | 3 | 1 | 1.03688 | 44.3 | 1.0 | 10718.3 | 999 | 999 | 999 | 43.7 | 1.6 | 6.4 · 10 ⁻¹⁶ |
| 8 | 90-303 23:09 | 0 | 1 | 140 | 4 | 9 | 0 | 7 | 6 | 0 | 0 | 4 | 1 | 1.03858 | 44.8 | 1.1 | 10701.8 | 86 | 209 | 3 | 43.7 | 1.6 | 1.2 · 10 ⁻¹⁶ |
| 9 | 90-304 13:30 | 0 | 2 | 188 | 8 | 8 | 0 | 6 | 15 | 0 | 1 | 0 | 42 | 1.04148 | 45.6 | 1.1 | 10674.2 | 154 | 200 | -63 | 43.5 | 1.9 | 2.1 · 10 ⁻¹⁶ |
| 10 | 90-304 13:38 | 0 | 1 | 32 | 1 | 13 | 0 | 15 | 15 | 0 | 1 | 0 | 4 | 1.04148 | 45.6 | 1.1 | 10674.2 | 294 | 15 | 23 | 11.8 | 1.1 | 1.4 · 10 ⁻¹³ |
| 11 | 90-305 07:39 | 0 | 1 | 149 | 6 | 9 | 0 | 6 | 15 | 0 | 1 | 0 | 43 | 1.04508 | 46.5 | 1.1 | 10641.1 | 99 | 207 | -8 | 10.0 | 5.4 | 2.5 · 10 ⁻¹³ |
| 12 | 90-305 13:46 | 0 | 2 | 50 | 12 | 20 | 0 | 7 | 8 | 5 | 0 | 0 | 33 | 1.04631 | 46.8 | 1.1 | 10630.0 | 999 | 999 | 999 | 34.1 | 1.9 | 5.2 · 10 ⁻¹⁴ |
| 13 | 90-306 08:18 | 0 | 2 | 187 | 8 | 15 | 0 | 7 | 0 | 6 | 0 | 0 | 4 | 1.05007 | 47.8 | 1.1 | 10597.0 | 152 | 201 | -61 | 34.1 | 1.9 | 1.7 · 10 ⁻¹⁴ |
| 14 | 90-306 10:04 | 0 | 1 | 68 | 1 | 7 | 0 | 15 | 7 | 11 | 0 | 0 | 3 | 1.05070 | 47.9 | 1.1 | 10591.5 | 345 | 345 | 70 | 56.0 | 2.0 | 1.8 · 10 ⁻¹⁶ |
| 15 | 90-306 10:42 | 0 | 2 | 105 | 3 | 10 | 0 | 8 | 6 | 8 | 0 | 0 | 4 | 1.05070 | 47.9 | 1.1 | 10591.5 | 37 | 221 | 51 | 43.5 | 1.9 | 6.2 · 10 ⁻¹⁶ |
| 16 | 90-306 11:51 | 0 | 1 | 105 | 3 | 10 | 0 | 8 | 6 | 8 | 0 | 0 | 3 | 1.05070 | 47.9 | 1.1 | 10591.5 | 37 | 221 | 51 | 21.4 | 1.9 | 1.7 · 10 ⁻¹⁴ |
| 17 | 90-306 13:25 | 0 | 1 | 105 | 2 | 9 | 0 | 9 | 6 | 7 | 0 | 0 | 3 | 1.05135 | 48.1 | 1.2 | 10586.0 | 999 | 999 | 999 | 11.8 | 11.8 | 8.4 · 10 ⁻¹⁴ |
| 18 | 90-307 21:40 | 0 | 1 | 127 | 4 | 4 | 0 | 7 | 15 | 0 | 1 | 0 | 3 | 1.05862 | 49.7 | 1.2 | 10525.5 | 67 | 211 | 22 | 34.1 | 1.9 | 4.4 · 10 ⁻¹⁶ |
| 19 | 90-308 00:43 | 0 | 1 | 165 | 3 | 9 | 0 | 8 | 6 | 8 | 0 | 0 | 5 | 1.05930 | 49.9 | 1.2 | 10520.1 | 120 | 203 | -30 | 38.7 | 1.6 | 1.7 · 10 ⁻¹⁶ |
| 20 | 90-308 19:50 | 0 | 3 | 149 | 19 | 25 | 0 | 7 | 5 | 6 | 0 | 0 | 45 | 1.06344 | 50.8 | 1.2 | 10487.2 | 98 | 206 | -7 | 28.1 | 1.6 | 4.4 · 10 ⁻¹³ |
| 21 | 90-308 20:24 | 0 | 2 | 68 | 11 | 14 | 0 | 14 | 15 | 0 | 1 | 0 | 2 | 1.06344 | 50.8 | 1.2 | 10487.2 | 344 | 345 | 70 | 2.1 | 1.6 | 2.0 · 10 ⁻¹⁰ |
| 22 | 90-310 01:00 | 0 | 1 | 48 | 3 | 13 | 0 | 8 | 15 | 0 | 1 | 0 | 47 | 1.07061 | 52.3 | 1.3 | 10432.5 | 999 | 999 | 999 | 21.4 | 1.9 | 2.8 · 10 ⁻¹⁴ |
| 23 | 90-310 02:09 | 0 | 1 | 88 | 3 | 17 | 0 | 7 | 15 | 11 | 0 | 0 | 33 | 1.07061 | 52.3 | 1.3 | 10432.5 | 12 | 249 | 73 | 34.1 | 1.9 | 4.3 · 10 ⁻¹⁶ |
| 24 | 90-310 13:24 | 0 | 1 | 56 | 4 | 17 | 0 | 8 | 15 | 10 | 0 | 0 | 33 | 1.07356 | 52.9 | 1.3 | 10410.6 | 377 | 2 | 55 | 21.4 | 1.9 | 7.2 · 10 ⁻¹⁴ |
| 25 | 90-311 03:12 | 0 | 1 | 111 | 1 | 15 | 0 | 15 | 0 | 1 | 0 | 1 | 0 | 1.07732 | 53.6 | 1.3 | 10383.4 | 44 | 217 | 44 | 11.8 | 11.8 | 1.8 · 10 ⁻¹³ |
| 26 | 90-311 07:15 | 0 | 1 | 15 | 4 | 10 | 0 | 7 | 6 | 7 | 0 | 0 | 3 | 1.07808 | 53.7 | 1.3 | 10377.9 | 999 | 999 | 999 | 48.9 | 1.6 | 9.0 · 10 ⁻¹⁶ |
| 27 | 90-311 13:43 | 0 | 1 | 153 | 3 | 9 | 0 | 8 | 7 | 8 | 0 | 0 | 2 | 1.07961 | 54.0 | 1.3 | 10367.0 | 999 | 999 | 999 | 34.6 | 1.6 | 2.7 · 10 ⁻¹⁶ |
| 28 | 90-312 21:22 | 0 | 1 | 8 | 3 | 19 | 0 | 6 | 15 | 0 | 1 | 0 | 47 | 1.08623 | 55.6 | 1.4 | 10307.3 | 259 | 19 | -11 | 43.5 | 1.9 | 3.3 · 10 ⁻¹⁶ |
| 29 | 90-312 23:30 | 0 | 1 | 145 | 1 | 5 | 0 | 15 | 7 | 6 | 0 | 0 | 3 | 1.08823 | 55.6 | 1.4 | 10307.3 | 92 | 208 | -1 | 56.0 | 2.0 | 1.3 · 10 ⁻¹⁶ |
| 30 | 90-313 05:36 | 0 | 1 | 201 | 3 | 13 | 0 | 8 | 15 | 0 | 1 | 0 | 47 | 1.08984 | 55.9 | 1.4 | 10296.4 | 999 | 999 | 999 | 21.4 | 1.9 | 2.8 · 10 ⁻¹⁴ |
| 31 | 90-314 06:34 | 3 | 1 | 130 | 7 | 11 | 5 | 6 | 6 | 5 | 0 | 1 | 3 | 1.09720 | 57.2 | 1.4 | 10247.8 | 70 | 210 | 19 | 55.2 | 1.6 | 1.1 · 10 ⁻¹⁵ |
| 32 | 90-314 23:36 | 1 | 1 | 1 | 1 | 21 | 1 | 15 | 14 | 0 | 1 | 1 | 41 | 1.10138 | 57.9 | 1.4 | 10220.8 | 999 | 999 | 999 | 11.8 | 11.8 | 3.5 · 10 ⁻¹³ |
| 33 | 90-315 08:32 | 0 | 1 | 144 | 3 | 15 | 0 | 8 | 0 | 0 | 1 | 0 | 3 | 1.10393 | 58.3 | 1.4 | 10204.6 | 90 | 207 | 0 | 21.4 | 1.9 | 3.7 · 10 ⁻¹⁴ |
| 34 | 90-315 17:38 | 0 | 1 | 139 | 2 | 7 | 0 | 9 | 6 | 6 | 0 | 0 | 3 | 1.10650 | 58.7 | 1.4 | 10188.5 | 83 | 208 | 7 | 70.0 | 2.0 | 9.1 · 10 ⁻¹⁷ |
| 35 | 90-316 13:36 | 0 | 1 | 153 | 6 | 13 | 0 | 6 | 6 | 7 | 0 | 0 | 36 | 1.11258 | 59.6 | 1.5 | 10150.9 | 102 | 206 | -12 | 43.5 | 1.9 | 3.3 · 10 ⁻¹⁶ |
| 36 | 90-317 12:17 | 0 | 1 | 160 | 5 | 10 | 0 | 7 | 6 | 7 | 0 | 0 | 4 | 1.11969 | 60.7 | 1.5 | 10108.1 | 112 | 204 | -21 | 48.9 | 1.6 | 1.1 · 10 ⁻¹⁶ |
| 37 | 90-318 17:23 | 0 | 1 | 182 | 4 | 1 | 0 | 7 | 15 | 10 | 0 | 0 | 45 | 1.12788 | 61.9 | 1.5 | 10060.2 | 142 | 199 | -52 | 34.1 | 1.9 | 8.9 · 10 ⁻¹⁶ |
| 38 | 90-318 23:21 | 0 | 1 | 149 | 1 | 6 | 0 | 15 | 6 | 9 | 0 | 0 | 3 | 1.12973 | 62.2 | 1.5 | 10049.5 | 96 | 205 | -6 | 70.0 | 2.0 | 6.3 · 10 ⁻¹⁷ |
| 39 | 90-319 16:24 | 0 | 1 | 88 | 1 | 14 | 0 | 15 | 15 | 0 | 1 | 0 | 47 | 1.13532 | 63.0 | 1.5 | 10017.7 | 10 | 251 | 74 | 11.8 | 11.8 | 1.6 · 10 ⁻¹³ |
| 40 | 90-321 01:06 | 0 | 1 | 232 | 2 | 7 | 0 | 15 | 8 | 7 | 0 | 0 | 3 | 1.14581 | 64.4 | 1.6 | 9959.5 | 212 | 23 | -57 | 36.7 | 2.0 | 1.3 · 10 ⁻¹⁶ |
| 41 | 90-321 07:34 | 3 | 4 | 17 | 25 | 26 | 10 | 11 | 9 | 15 | 0 | 1 | 30 | 1.14774 | 64.7 | 1.6 | 9949.0 | 270 | 16 | 0 | 2.5 | 1.9 | 3.7 · 10 ⁻¹⁶ |
| 42 | 90-321 17:03 | 0 | 1 | 240 | 1 | 12 | 0 | 15 | 8 | 0 | 1 | 0 | 47 | 1.15066 | 65.1 | 1.6 | 9933.2 | 223 | 21 | -46 | 11.8 | 11.8 | 1.2 · 10 ⁻¹³ |
| 43 | 90-322 09:37 | 0 | 1 | 148 | 4 | 8 | 0 | 8 | 7 | 7 | 0 | 0 | 3 | 1.15656 | 65.8 | 1.6 | 9901.7 | 94 | 205 | -4 | 34.6 | 1.6 | 2.7 · 10 ⁻¹⁶ |
| 44 | 90-322 09:37 | 0 | 2 | 195 | 10 | 19 | 0 | 7 | 5 | 6 | 0 | 0 | 38 | 1.15656 | 65.8 | 1.6 | 9901.7 | 160 | 195 | -69 | 34.1 | 1.9 | 2.9 · 10 ⁻¹⁴ |
| 45 | 90-322 22:08 | 0 | 1 | 94 | 1 | 6 | 0 | 15 | 7 | 9 | 0 | 0 | 3 | 1.16054 | 66.3 | 1.6 | 9860.0 | 18 | 235 | 68 | 56.0 | 2.0 | 1.5 · 10 ⁻¹⁶ |
| 46 | 90-323 02:53 | 0 | 1 | 198 | 3 | 6 | 0 | 9 | 5 | 10 | 1 | 0 | 14 | 1.16154 | 66.5 | 1.6 | 9875.5 | 164 | 193 | -73 | 31.4 | 1.8 | 2.2 · 10 ⁻¹⁶ |
| 47 | 90-323 07:13 | 0 | 1 | 4 | 2 | 7 | 0 | 9 | 6 | 7 | 0 | 0 | 4 | 1.16354 | 66.7 | 1.6 | 9865.1 | 251 | 18 | -18 | 70.0 | 2.0 | 9.1 · 10 ⁻¹⁷ |
| 48 | 90-323 16:41 | 0 | 1 | 149 | 3 | 7 | 0 | 7 | 6 | 0 | 0 | 0 | 3 | 1.16657 | 67.1 | 1.6 | 9849.4 | 95 | 205 | -5 | 43.7 | 1.6 | 7.2 · 10 ⁻¹⁶ |
| 49 | 90-323 18:28 | 3 | 1 | 138 | 4 | 9 | 8 | 7 | 6 | 5 | 0 | 1 | 3 | 1.16758 | 67.2 | 1.6 | 9844.2 | 80 | 207 | 10 | 48.9 | 1.6 | 7.5 · 10 ⁻¹⁶ |
| 50 | 90-324 02:19 | 0 | 1 | 105 | 3 | 7 | 0 | 8 | 7 | 8 | 0 | 0 | 3 | 1.16961 | 67.5 | 1.6 | 9833.8 | 33 | 220 | 55 | 34.6 | 1.6 | 1.9 · 10 ⁻¹⁶ |

Table 4. (Continued)

Table with columns: No., IMP, DATE, C, AR, S, IA, EA, CA, IT, ET, E, I, C, PA, P, E, Y, I, E, C, P, HV, R, LON, LAT, D, Jap, ROT, S, Lon, SLAT, V, VEF, M, MEF. Contains multiple rows of astronomical data.

Table 4. (Continued)

| No. | IMP. | DATE | C | AR | S | IA | EA | CA | IT | ET | E | E | I | C | P | HV | R | Lon | LAT | D _{Jup} | ROT | S _{Lon} | S _{Lat} | V | V _{EF} | M | MEF | | | |
|-----|--------|-------|---|----|-----|----|----|----|----|----|----|---|---|----|----|----|---|---------|---------|------------------|--------|------------------|------------------|-----|-----------------|------|-----|-------------------|-------------------|------|
| 931 | 92-292 | 20:42 | 0 | 1 | 123 | 2 | 6 | 0 | 15 | 8 | 10 | 0 | 0 | 0 | 0 | 1 | 3 | 5.20240 | 159.8 | -11.6 | 4158.4 | 51 | 255 | 39 | 36.7 | 2.0 | 1.1 | 10 ⁻¹⁶ | 12.5 | |
| 932 | 92-292 | 23:41 | 0 | 1 | 138 | 6 | 11 | 0 | 7 | 7 | 6 | 0 | 0 | 0 | 0 | 1 | 3 | 5.20220 | 159.8 | -11.6 | 4160.3 | 73 | 259 | 18 | 43.7 | 1.6 | 2.3 | 10 ⁻¹⁶ | 6.0 | |
| 933 | 92-293 | 01:58 | 0 | 1 | 138 | 2 | 3 | 0 | 15 | 5 | 12 | 0 | 0 | 0 | 0 | 1 | 3 | 5.20200 | 159.8 | -11.7 | 4162.3 | 999 | 999 | 999 | 11.8 | 11.8 | 3.2 | 10 ⁻¹⁴ | 5858.3 | |
| 934 | 92-293 | 05:53 | 0 | 1 | 149 | 3 | 6 | 0 | 9 | 9 | 0 | 0 | 0 | 0 | 0 | 1 | 3 | 5.20181 | 159.8 | -11.7 | 4164.2 | 88 | 261 | 3 | 21.0 | 1.6 | 9.3 | 10 ⁻¹⁶ | 6.0 | |
| 935 | 92-294 | 08:12 | 0 | 1 | 58 | 4 | 7 | 0 | 9 | 8 | 8 | 0 | 0 | 0 | 0 | 1 | 3 | 5.20001 | 159.8 | -11.7 | 4181.8 | 319 | 81 | 49 | 22.7 | 1.6 | 9.1 | 10 ⁻¹⁶ | 6.0 | |
| 936 | 92-294 | 16:49 | 3 | 1 | 114 | 2 | 6 | 1 | 9 | 8 | 9 | 0 | 0 | 0 | 0 | 1 | 3 | 5.19942 | 159.8 | -11.7 | 4187.6 | 41 | 253 | 49 | 36.7 | 2.0 | 1.1 | 10 ⁻¹⁶ | 12.5 | |
| 937 | 92-295 | 20:48 | 0 | 1 | 115 | 3 | 6 | 0 | 8 | 8 | 8 | 0 | 0 | 0 | 0 | 1 | 3 | 5.19761 | 159.8 | -11.8 | 4205.1 | 42 | 253 | 48 | 28.0 | 1.6 | 3.1 | 10 ⁻¹⁶ | 6.0 | |
| 938 | 92-295 | 22:34 | 3 | 1 | 202 | 5 | 9 | 3 | 7 | 7 | 7 | 0 | 0 | 0 | 0 | 1 | 3 | 5.19741 | 159.8 | -11.8 | 4207.1 | 999 | 999 | 999 | 43.7 | 1.6 | 1.4 | 10 ⁻¹⁶ | 6.0 | |
| 939 | 92-296 | 06:50 | 1 | 2 | 148 | 13 | 13 | 11 | 10 | 9 | 0 | 1 | 1 | 6 | 31 | 1 | 3 | 5.19681 | 159.8 | -11.8 | 4212.9 | 88 | 262 | 3 | 10.4 | 1.9 | 1.4 | 10 ⁻¹² | 10.5 | |
| 940 | 92-296 | 16:11 | 0 | 2 | 188 | 8 | 9 | 0 | 11 | 15 | 0 | 1 | 0 | 0 | 0 | 1 | 3 | 5.19621 | 159.8 | -11.8 | 4218.7 | 144 | 279 | -50 | 7.8 | 1.9 | 7.1 | 10 ⁻¹³ | 10.5 | |
| 941 | 92-301 | 07:01 | 3 | 1 | 142 | 5 | 10 | 2 | 7 | 7 | 7 | 0 | 1 | 0 | 0 | 0 | 1 | 3 | 5.18669 | 159.9 | -12.1 | 4290.6 | 81 | 261 | 10 | 43.7 | 1.6 | 1.7 | 10 ⁻¹⁶ | 6.0 |
| 942 | 92-302 | 09:09 | 3 | 2 | 180 | 10 | 19 | 14 | 8 | 8 | 9 | 0 | 1 | 36 | 0 | 1 | 3 | 5.18684 | 159.9 | -12.1 | 4308.1 | 134 | 275 | -41 | 21.4 | 1.9 | 1.5 | 10 ⁻¹³ | 10.5 | |
| 943 | 92-304 | 19:13 | 3 | 3 | 149 | 20 | 25 | 4 | 6 | 6 | 6 | 0 | 1 | 44 | 0 | 1 | 3 | 5.18290 | 159.9 | -12.3 | 4344.9 | 92 | 264 | 0 | 28.0 | 1.6 | 5.9 | 10 ⁻¹⁴ | 6.0 | |
| 944 | 92-309 | 13:17 | 0 | 1 | 111 | 3 | 2 | 0 | 11 | 13 | 0 | 1 | 0 | 35 | 21 | 1 | 3 | 5.17493 | 159.9 | -12.5 | 4418.4 | 39 | 253 | 51 | 7.8 | 1.9 | 9.5 | 10 ⁻¹⁴ | 10.5 | |
| 945 | 92-310 | 17:52 | 3 | 3 | 124 | 20 | 26 | 17 | 5 | 5 | 5 | 0 | 1 | 46 | 0 | 1 | 3 | 5.17302 | 160.0 | -12.6 | 4435.8 | 57 | 257 | 34 | 43.7 | 1.6 | 1.4 | 10 ⁻¹³ | 6.0 | |
| 946 | 92-310 | 18:43 | 3 | 2 | 150 | 14 | 21 | 11 | 8 | 9 | 6 | 0 | 1 | 39 | 0 | 1 | 3 | 5.17280 | 160.0 | -12.6 | 4437.7 | 93 | 264 | -1 | 21.4 | 1.9 | 4.2 | 10 ⁻¹³ | 10.5 | |
| 947 | 92-311 | 13:21 | 1 | 1 | 129 | 3 | 2 | 3 | 10 | 11 | 0 | 1 | 1 | 0 | 0 | 0 | 1 | 3 | 5.17153 | 160.0 | -12.6 | 4449.3 | 65 | 259 | 25 | 10.4 | 1.9 | 4.4 | 10 ⁻¹⁴ | 10.5 |
| 948 | 92-312 | 13:10 | 0 | 1 | 204 | 2 | 4 | 0 | 12 | 11 | 0 | 1 | 0 | 0 | 0 | 1 | 3 | 5.16982 | 160.0 | -12.7 | 4464.8 | 171 | 319 | -70 | 11.8 | 11.8 | 3.6 | 10 ⁻¹⁴ | 5858.3 | |
| 949 | 92-318 | 07:13 | 1 | 2 | 134 | 9 | 6 | 10 | 9 | 15 | 0 | 1 | 1 | 12 | 24 | 1 | 3 | 5.15985 | 160.0 | -13.0 | 4553.3 | 72 | 261 | 18 | 14.1 | 1.9 | 1.1 | 10 ⁻¹³ | 10.5 | |
| 950 | 92-319 | 17:28 | 3 | 2 | 106 | 14 | 22 | 12 | 8 | 6 | 6 | 0 | 1 | 40 | 0 | 1 | 3 | 5.15744 | 160.0 | -13.1 | 4574.5 | 35 | 251 | 55 | 21.4 | 1.9 | 5.0 | 10 ⁻¹³ | 10.5 | |
| 951 | 92-320 | 10:50 | 1 | 1 | 173 | 5 | 1 | 8 | 9 | 8 | 0 | 1 | 1 | 4 | 24 | 1 | 3 | 5.15612 | 160.1 | -13.1 | 4586.0 | 129 | 276 | -35 | 14.1 | 1.9 | 2.5 | 10 ⁻¹⁴ | 10.5 | |
| 952 | 92-321 | 15:48 | 3 | 2 | 15 | 9 | 14 | 21 | 8 | 9 | 7 | 0 | 1 | 0 | 0 | 0 | 1 | 3 | 5.15391 | 160.1 | -13.2 | 4605.2 | 999 | 999 | 999 | 25.9 | 1.6 | 4.4 | 10 ⁻¹⁴ | 6.0 |
| 953 | 92-325 | 07:48 | 3 | 2 | 125 | 9 | 14 | 1 | 8 | 8 | 9 | 0 | 1 | 38 | 0 | 1 | 3 | 5.14564 | 160.1 | -13.4 | 4676.1 | 999 | 999 | 999 | 28.0 | 1.6 | 3.3 | 10 ⁻¹⁴ | 6.0 | |
| 954 | 92-328 | 20:44 | 3 | 2 | 100 | 12 | 20 | 6 | 8 | 7 | 7 | 0 | 1 | 38 | 0 | 1 | 3 | 5.14111 | 160.1 | -13.5 | 4714.3 | 27 | 247 | 62 | 21.4 | 1.9 | 2.6 | 10 ⁻¹³ | 10.5 | |
| 955 | 92-330 | 02:45 | 0 | 1 | 192 | 2 | 1 | 0 | 15 | 15 | 0 | 1 | 0 | 14 | 31 | 1 | 3 | 5.13883 | 160.2 | -13.6 | 4733.4 | 156 | 297 | -59 | 11.8 | 11.8 | 2.4 | 10 ⁻¹⁴ | 5858.3 | |
| 956 | 92-330 | 14:51 | 3 | 2 | 164 | 11 | 20 | 7 | 8 | 5 | 7 | 0 | 1 | 38 | 0 | 1 | 3 | 5.13792 | 160.2 | -13.6 | 4741.1 | 117 | 273 | -24 | 21.4 | 1.9 | 2.2 | 10 ⁻¹³ | 10.5 | |
| 957 | 92-335 | 07:39 | 3 | 3 | 48 | 14 | 22 | 27 | 7 | 6 | 6 | 0 | 1 | 41 | 0 | 1 | 3 | 5.12915 | 160.2 | -13.9 | 4813.5 | 999 | 999 | 999 | 34.1 | 1.9 | 9.7 | 10 ⁻¹³ | 10.5 | |
| 958 | 92-338 | 10:45 | 3 | 3 | 86 | 19 | 22 | 13 | 7 | 6 | 6 | 0 | 1 | 41 | 0 | 1 | 3 | 5.12330 | 160.3 | -14.1 | 4861.0 | 999 | 999 | 999 | 22.7 | 1.6 | 5.8 | 10 ⁻¹³ | 6.0 | |
| 959 | 92-339 | 15:03 | 3 | 3 | 222 | 19 | 22 | 7 | 6 | 6 | 5 | 0 | 1 | 41 | 0 | 1 | 3 | 5.12094 | 160.3 | -14.1 | 4880.0 | 201 | 40 | -61 | 28.0 | 1.6 | 2.8 | 10 ⁻¹⁴ | 6.0 | |
| 960 | 92-346 | 04:56 | 1 | 1 | 127 | 7 | 15 | 7 | 8 | 0 | 10 | 0 | 1 | 6 | 31 | 1 | 3 | 5.10851 | 160.3 | -14.5 | 4978.6 | 69 | 262 | 21 | 21.4 | 1.9 | 7.2 | 10 ⁻¹⁴ | 10.5 | |
| 961 | 92-347 | 14:34 | 0 | 2 | 222 | 9 | 13 | 0 | 7 | 8 | 6 | 0 | 0 | 35 | 0 | 1 | 3 | 5.10584 | 160.4 | -14.6 | 4999.3 | 203 | 42 | -59 | 35.4 | 1.6 | 1.3 | 10 ⁻¹³ | 6.0 | |
| 962 | 92-348 | 08:44 | 2 | 2 | 120 | 10 | 19 | 11 | 8 | 6 | 6 | 0 | 1 | 37 | 0 | 1 | 3 | 5.10439 | 160.4 | -14.6 | 5010.7 | 59 | 259 | 31 | 21.4 | 1.9 | 1.5 | 10 ⁻¹³ | 10.5 | |
| 963 | 92-349 | 21:47 | 3 | 2 | 185 | 12 | 19 | 11 | 11 | 9 | 8 | 0 | 1 | 10 | 31 | 1 | 3 | 5.10121 | 160.4 | -14.7 | 5035.2 | 153 | 297 | -55 | 7.8 | 1.9 | 4.1 | 10 ⁻¹² | 10.5 | |
| 964 | 92-354 | 19:18 | 3 | 1 | 88 | 1 | 2 | 1 | 15 | 15 | 4 | 0 | 1 | 6 | 31 | 1 | 3 | 5.09159 | 160.4 | -15.0 | 5108.7 | 17 | 231 | 70 | 11.8 | 11.8 | 2.3 | 10 ⁻¹⁴ | 5858.3 | |
| 965 | 92-357 | 07:47 | 3 | 2 | 187 | 8 | 12 | 7 | 9 | 10 | 10 | 0 | 1 | 0 | 0 | 1 | 3 | 5.08659 | 160.5 | -15.1 | 5146.2 | 999 | 999 | 999 | 19.3 | 1.6 | 8.8 | 10 ⁻¹⁴ | 6.0 | |
| 966 | 92-362 | 18:38 | 0 | 1 | 165 | 5 | 22 | 0 | 10 | 4 | 13 | 0 | 0 | 5 | 24 | 1 | 3 | 5.07546 | 160.5 | -15.4 | 5228.7 | 128 | 280 | -34 | 10.4 | 1.9 | 1.1 | 10 ⁻¹² | 10.5 | |
| 967 | 92-363 | 16:34 | 3 | 2 | 176 | 11 | 20 | 4 | 8 | 5 | 7 | 0 | 1 | 38 | 0 | 1 | 3 | 5.07367 | 160.5 | -15.4 | 5241.8 | 144 | 280 | -47 | 21.4 | 1.9 | 2.2 | 10 ⁻¹³ | 10.5 | |
| 968 | 92-364 | 01:06 | 3 | 2 | 142 | 14 | 21 | 13 | 7 | 6 | 6 | 0 | 1 | 40 | 0 | 1 | 3 | 5.07290 | 160.5 | -15.5 | 5247.4 | 96 | 268 | -3 | 34.1 | 1.9 | 8.3 | 10 ⁻¹⁴ | 10.5 | |

numbers (IA, EA, CA) and rise times (IT, ET), time difference and coincidence of electron and ion signals (EIT, EIC), coincidence of ion and channeltron signal (IIC), and charge reading at the entrance grid (PA) as well as time (PET) between this signal and the impact. This is followed by instrument status information such as event definition (EVD), charge sensing thresholds (ICP, ECP, CCP, PCP) and channeltron high voltage level (HV, see Paper I for further explanations).

Information about the orbit of the spacecraft follows next: heliocentric distance (R) in AU, ecliptic longitude and latitude (LON, LAT) and distance to Jupiter (R_J). The coordinate system used throughout is the ecliptic system with the Earth mean ecliptic and equinox of 1950.0. The rotation angle (ROT) specifies the angular orientation of the spacecraft about its spin axis at the time of each impact. It is measured in the plane perpendicular to the spin axis of *Ulysses* which points roughly toward the Earth. The angle ROT is defined to be zero when the dust sensor looks closest to the ecliptic north and it increases as *Ulysses* rotates positively about its spin axis. Whenever the SEC is not valid, a value of 999 is given (this occurs 147 times). Ecliptic longitude and latitude (S_{LON} , S_{LAT}) of the sensor axis at time of impact are displayed next. (If ROT is not valid, then S_{LON} and S_{LAT} are not either.) Mean impact speed (v) and speed error factor (VEF) as well as mean particle mass (m) and mass error factor (MEF) are presented last. We suggest that whenever $VEF > 6$, both speed and mass values should be discarded (this occurs for 86 impacts).

The *Ulysses* dust instrument is also capable of measuring the charge of a dust grain just before it strikes the sensor. No values are given here because the frequency and amplitude of noise events on the induced charge grid are very high (see Paper I). We hope to obtain reliable dust charge values for at least some of the dust impacts after careful study of the noise environment.

Analysis

In this section we discuss important technical aspects of the *Ulysses* detector. We present simple expressions for the detection threshold of impacting particles and for the boundary between what we call “big” and “small” impacts. These considerations are useful for understanding the completeness of both the *Ulysses* and *Galileo* dust data sets and for comparing them.

Because of its relative insensitivity to noise, the signal arising from positively charged ions created during the impact Q_i , is the most important impact parameter determined by the *Ulysses* dust detector. Figure 4 shows the differential distribution of impact charges measured up to the end of 1992. Impact-generated ions are observed over the entire calibrated range, and only a few impacts are close to the saturation limit of $Q_i \sim 10^{-8}$ C. Since the number of impacts with large Q_i values drops off rapidly (roughly a power law with index about -1.2), it appears that there are no severe saturation effects. The curve may flatten out somewhat at the lowest Q_i values, possibly indicating that the sensitivity threshold is smeared out

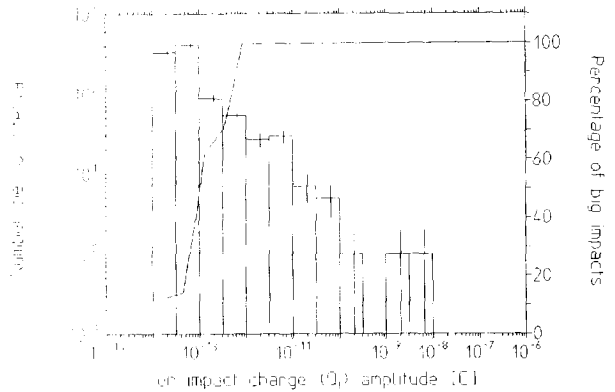


Fig. 4. Distribution of the ion signal amplitude. The dashed histogram gives the distribution of “big” impacts and the solid histogram gives all impacts. The curve shows the contribution of “big” impacts, defined in the text, to the total number of impacts

rather than sharp. If this is the case, then the number of the smallest impact charges is not complete.

The channeltron picks up a portion of the ions generated by a dust impact and amplifies the resulting signal. Coincident detections of Q_i and channeltron pulses provide a strong criterion for separating true dust impacts from noise events; this separates class 0 events (mostly noise) from the higher classes (mostly impacts)—see Paper I. After launch of both *Galileo* and *Ulysses*, it was found that the channeltron was much more sensitive to noise than expected from preflight laboratory tests. It is important, therefore, to characterize its in-flight performance. A good measure of the channeltron amplification A is the ratio of the channeltron charge Q_c to the ion charge Q_i . This ratio is displayed in Fig. 5 as a function of the ion charge Q_i (at channeltron high voltage step HV = 3, i.e. 1140 V). The sensitivity threshold and saturation limits of the channeltron charge can be approximated by 1.0×10^{-13} and 1.7×10^{-9} C, respectively. The mean amplification at this high voltage setting is $A \sim 2.2$. As can be seen in Fig. 5, however, the ion charge and the

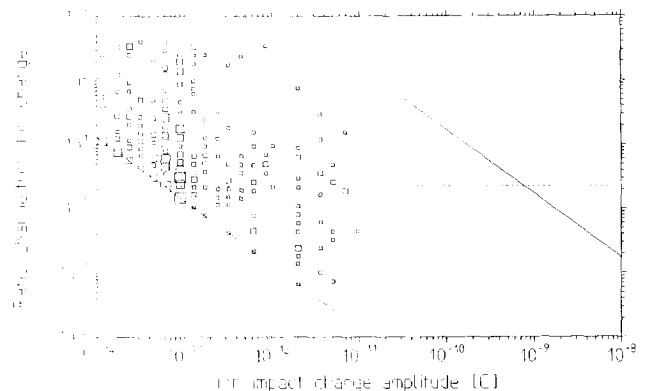


Fig. 5. Channeltron amplification $A = Q_c/Q_i$, i.e. ratio of the channeltron charge amplitude to the ion grid charge for a channeltron high voltage of 1140 V (HV = 3). The solid lines denote the sensitivity threshold and saturation limit of the channeltron. The dotted line shows the mean value of the channeltron amplification $A = 2.2$ for ion impact charges 10^{-13} C $< Q_i < 10^{-11}$ C. Boxes indicate dust particle impacts; the area of each box is proportional to the number of impacts included

channeltron output are not tightly correlated due to the statistics of impacting particles. It can be seen that for ion grid charges less than about 10^{-12} C, impacts with no measurable channeltron charge can be expected. In these cases, other signal criteria have to be used to decide whether an event is a true dust impact. Note that no impacts with $Q_1 > 10^{-11}$ C were recorded while HV was set to step 3.

The impact charge, Q_1 , characterizes the amplitude range of a recorded event. Together with the class number, which indicates how “impact-like” an event is, the category of an event is determined. Events classified in all other categories except AC01, AC11 and AC02 have been found almost exclusively to be true dust impacts—we will call them “big” impacts. “Small” impacts are more difficult to identify as they must be carefully separated from noise events (Baguhl *et al.*, 1994). It must be emphasized that “big” and “small” impacts are *not* classified according to their masses, but according to the amplitude of the ion grid signal (AR) and a set of conditions imposed on the signal parameters (described by the CLN number)—see Paper I. Masses and speeds of “big” impacts recorded until the end of 1992 are displayed in Fig. 6a; the same is shown for “small” impacts in Fig. 6b. “Small”

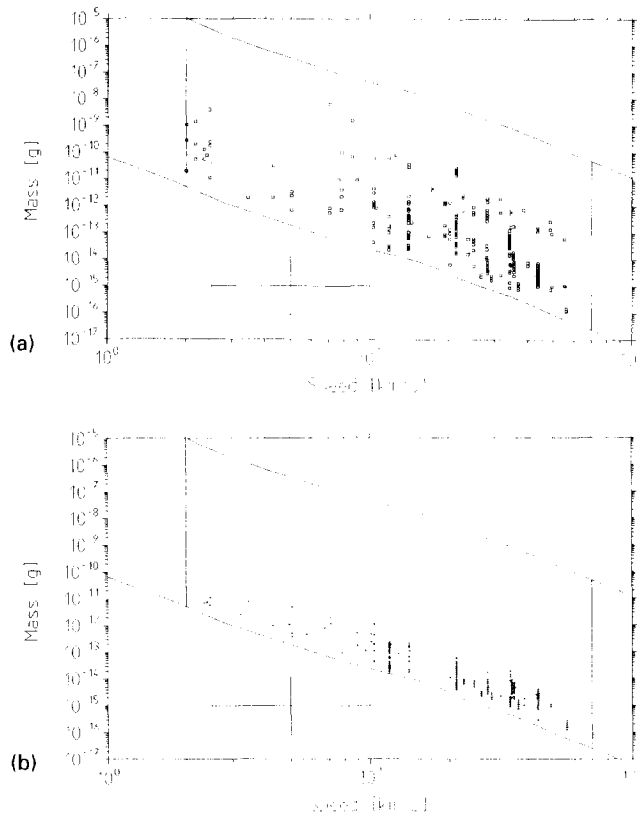


Fig. 6. Particle masses and speeds of “big” impacts (a) and “small” impacts (b). The solid line encloses the sensor’s sensitivity region. A sample error bar indicating typical errors of plus or minus a factor of two in velocity and a factor of ten in mass is shown. The clustering of the speed values stems from the discrete steps in the ion and electron signal rise times, but these errors are much smaller than the nominal factor of two speed errors. The broken line shows the effective division between “big” and “small” impacts (cf. Fig. 7)

impacts are restricted to a band of width a factor one hundred in mass above the sensitivity threshold. About 80% of all “big” impacts are found there as well. Speeds have been found over the entire calibrated range from 2 to 70 km s^{-1} and the masses vary over 8 orders of magnitude from 6×10^{-17} to 6×10^{-9} g.

First, we determine the effective threshold for the detection of an impact. The smallest impact charge Q_1 detectable is about 10^{-14} C which corresponds to a mass and speed dependent threshold that can be approximated by a power law:

$$\frac{m_{\text{th}}}{1 \text{ g}} = 1.2 \times 10^{-10} \left(\frac{v}{1 \text{ km s}^{-1}} \right)^{-3.4} \quad (1)$$

where m_{th} is the particle mass and v the impact speed. This is simply an analytic approximation to the lower limit shown in Figs 6a and b, which may deviate from the actual values by up to a factor of 2. In order to calculate a mass threshold which is independent of speed, the speed distribution of the impacting particles has to be known or assumed. For example, if we ignore particles which strike *Ulysses* at speeds below 6 km s^{-1} ($\sim 5\%$ of all particles), then a meaningful mass threshold of $> 2 \times 10^{-13}$ g (as obtained from equation (1) or Fig. 6) can be used. At this mass, all particles except the slowest ($< 6 \text{ km s}^{-1}$) can be detected and hence for rapidly-moving particles the data set is complete.

Now, we determine the division between “big” and “small” impacts. There exists no sharp boundary in Fig. 6 between “big” and “small” impacts, because these names are defined in terms of ion and channeltron signals. This can also be seen in Fig. 4, which shows the contribution of “big” impacts to the total number of impacts as a function of impact charge. “Big” impacts (solid line), which constitute about 35% of all impacts, persist at even the smallest impact charges. Nevertheless, a sensible division between big and small impacts can be defined at a given impact speed: we choose the mass at which the number of all impacts (“big” or “small”) with greater masses equals the total number of “big” impacts. This guarantees that an impact rate calculated from only the “big” impacts will give the correct impact rate for all particles detected by the sensor above that threshold mass. The resulting threshold, which is a function of speed, is plotted in Fig. 7 for a channeltron high voltage of 1140 V (HV 3). The best fit for the separation between “big” and “small” impacts can be approximated by

$$\frac{m_{\text{bs}}}{1 \text{ g}} = k \left(\frac{v}{1 \text{ km s}^{-1}} \right)^{-3.4} \quad (2)$$

where m_{bs} is the velocity dependent mass separating “big” and “small” impacts, v is the impact speed and k a constant of 8.9×10^{-10} for 1140 V (HV 3) and 1.1×10^{-9} for 1020 V (HV 2). Although this calculation helps us to understand the *Ulysses* measurements, it is especially important for the *Galileo* experiment which could only register “big” impacts during most of its mission.

Discussion

The impact rate measured by the *Ulysses* dust detector through 1992 is displayed in Fig. 8. Impact rates for both

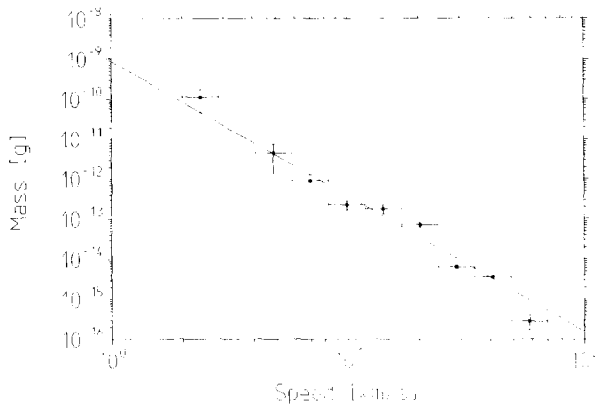


Fig. 7. Speed dependent mass threshold dividing “big” and “small” impacts for a high voltage of 1140 V. The data points are plotted so at a given velocity, the total number of “big” dust impacts equals the number of all impacts, “big” and “small”, above the point. The solid line is a best fit of the form $m = av^b$ in which the exponent b has been set to -3.4 . This choice of exponent corresponds to a constant impact charge Q_i (cf. equation (1))

“big” impacts identified by the speed dependent mass threshold just derived, and all particles are shown. These data are believed to contain no noise events (cf. Baguhl *et al.*, 1993). Except for the Jupiter flyby and some of the dust streams, the flux of “big” impacts varies only slowly and remains low (~ 0.5 impacts per day).

During the initial 2 months of the *Ulysses* mission, the impact of all dust particles decreased by about one order of magnitude (Fig. 8). This may be due to high speed and low angular momentum β -meteoroids which could enter the sensor only during this period. Alternatively, the effect may arise from interstellar particles, the flux of which should be strongly enhanced over this part of the *Ulysses* orbit due to gravitational focusing by the Sun. These particles, however, would have to reach *Ulysses*’ position at about 1.2 AU without sublimating. During about six months around Jupiter flyby, the rate of “small” impacts fluctuated dramatically and periodically. Periods of about 15 and 28 days between flux peaks were observed prior to and after Jupiter flyby, respectively. The increases are

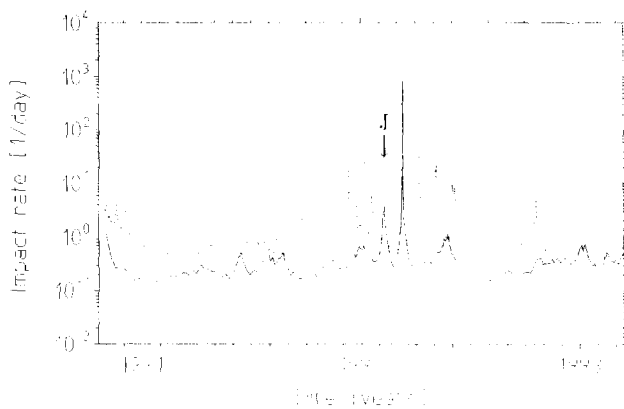


Fig. 8. Dust impact rate vs time. The dashed line gives the rate of all particles while the solid line shows only “big” impacts with masses greater than that defined by equation (2). A sliding mean over eight impacts was applied to the data. The “J” indicates the time of the Jupiter flyby

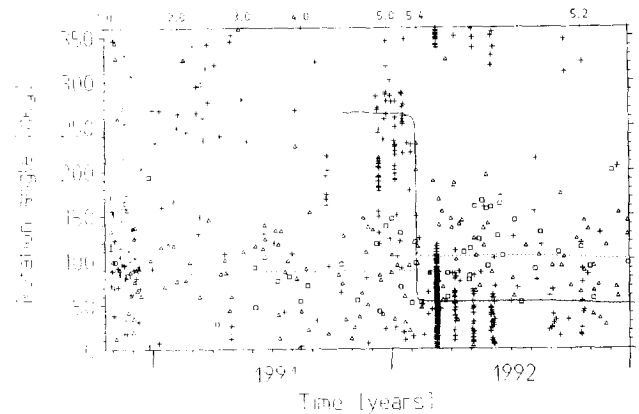


Fig. 9. Rotation angle vs time. Symbols are chosen according to different combinations of masses and speeds. Squares denote speeds larger than 26 km s^{-1} and triangles indicate slower particles; both symbols refer to particles with masses above $2.5 \times 10^{-14} \text{ g}$. Plus signs mark particles with masses $\leq 2.5 \times 10^{-14} \text{ g}$. The direction to Jupiter (solid line) and to the upstream direction of the interstellar gas flow (dashed line) are shown. The heliocentric distance of *Ulysses* from the Sun is given in the upper scale

attributed to dust streams originating from the jovian system (Grün *et al.*, 1993; Baguhl *et al.*, 1994).

The rotation angle of dust impacts versus time is displayed in Fig. 9. For comparison, the direction to Jupiter

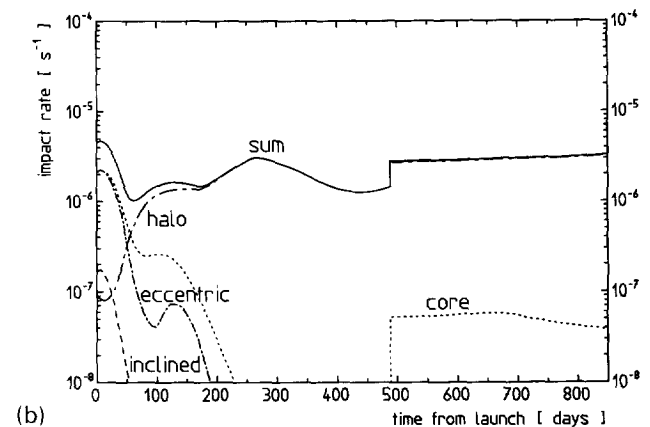
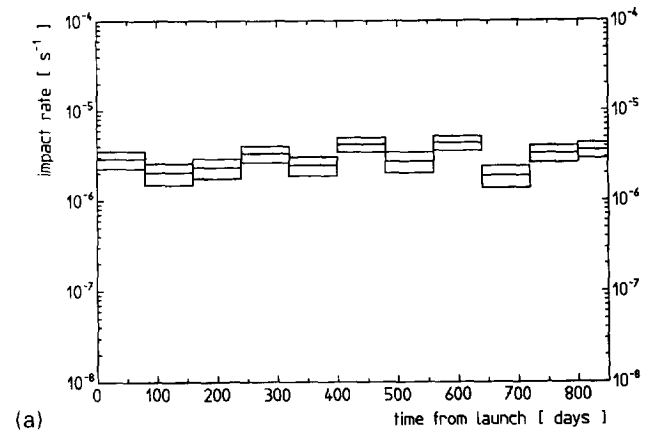


Fig. 10. Comparison of (a) the measured impact rate (“big” impacts only) with (b) the dust model of Divine (1993). Jupiter flyby and stream particles were removed from the data set since these are not considered by the model. The different populations and their sum are shown separately

and the upstream direction of the local interstellar medium are shown too. A discussion of this data can be found in Baguhl *et al.* (1993) and Grün *et al.* (1994).

Divine's (1993) "Five populations of interplanetary meteoroids" is based on a variety of interplanetary dust observations including initial *Ulysses* data from the first year of the mission. This empirical model allows us to predict the impact rate for a dust detector of known characteristics (geometry, mass and speed sensitivity). It is of interest to compare the measured impact rates (Fig. 10a) with the model values (Fig. 10b). Except for the first 50 days of the mission, the impact rates are dominated by Divine's halo population which had been specifically constructed to fit the *Pioneer* 10 and 11 penetration data (Humes, 1980). This population is assumed to have orbits of random inclinations and moderate eccentricities. While the general magnitude of the flux is well represented, specific features of the model (like the factor of two increase in the flux after Jupiter) are not found in the data. In addition, *Ulysses* data (Grün *et al.*, 1992d, 1993) clearly shows that the dust flux at Jupiter's distance is not compatible with random inclinations—at the position of *Ulysses* the measured flux is predominantly retrograde. It has been concluded (Grün *et al.*, 1993, 1994; Baguhl *et al.*, 1994) that this flux is due primarily to interstellar particles penetrating the solar system to within at least 3 AU of the Sun. To match the findings of *Ulysses*, the halo population in Divine's model must be significantly altered and perhaps eliminated altogether in favor of an interstellar population.

References

- Baguhl, M., Identifikation von Staubeinschlägen in den Daten der Mikrometeoroiden-Detektoren an Bord der Raumsonden *Ulysses* und *Galileo*. Ph.D. thesis, University of Heidelberg, 1993.
- Baguhl, M., Grün, E., Linkert, D., Linkert, G. and Siddique, N., Performance of the *Galileo* and *Ulysses* dust detectors. *Proceeding of the Workshop on Hypervelocity Impacts in Space* (edited by J. A. M. McDonnell), pp. 153–159. University of Kent at Canterbury, 1992.
- Baguhl, M., Grün, E., Linkert, D., Linkert, G. and Siddique, N., Identification of 'small' dust impacts in the *Ulysses* dust detector data. *Planet. Space Sci.* **41**, 1085–1098, 1993.
- Baguhl, M., Grün, E., Hamilton, D. P., Linkert, G., Riemann, R., Staubach, P. and Zook, H., The flux of interstellar dust observed by *Ulysses* and *Galileo*. *Space Sci. Rev.* **72**, 471–476, 1994.
- Divine, N., Five populations of interplanetary meteoroids. *J. geophys. Res.* **98**, 17029–17048, 1993.
- Grün, E., Fechtig, H., Giese, R. H., Kissel, J., Linkert, D., Maas, D., McDonnell, J. A. M., Morfill, G. E., Schwehm, G. and Zook, H. A., The *Ulysses* dust experiment. *Astron. Astrophys. Suppl. Ser.* **92**, 411–423, 1992a.
- Grün, E., Fechtig, H., Hanner, M. S., Kissel, J., Lindblad, B.-A., Linkert, D., Linkert, G., Morfill, G. E. and Zook, H. A., The *Galileo* dust detector. *Space Sci. Rev.* **60**, 317–340, 1992b.
- Grün, E., Baguhl, M., Fechtig, H., Hanner, M. S., Kissel, J., Lindblad, B.-A., Linkert, D., Linkert, G., McDonnell, J. A. M., Morfill, G. E., Schwehm, G., Siddique, N. and Zook, A., Interplanetary dust near 1 AU. *Proceeding of the Workshop on Hypervelocity Impacts in Space* (edited by J. A. M. McDonnell), pp. 173–179. University of Kent at Canterbury, 1992c.
- Grün, E., Baguhl, M., Fechtig, H., Hanner, M. S., Kissel, J., Lindblad, B.-A., Linkert, D., Linkert, G., Mann, I., McDonnell, J. A. M., Morfill, G. E., Polanskey, C., Riemann, R., Schwehm, G., Siddique, N. and Zook, H. A., *Galileo* and *Ulysses* dust measurements: from Venus to Jupiter. *Geophys. Res. Lett.* **19**, 1311–1314, 1992d.
- Grün, E., Zook, H. A., Baguhl, M., Fechtig, H., Hanner, M. S., Kissel, J., Lindblad, B.-A., Linkert, D., Linkert, G., Mann, I., McDonnell, J. A. M., Morfill, G. E., Planskey, C., Riemann, R., Schwehm, G. and Siddique, N., *Ulysses* dust measurements near Jupiter. *Science* **257**, 1550–1552, 1992e.
- Grün, E., Zook, H. A., Baguhl, M., Balogh, A., Bame, S. J., Fechtig, H., Forsyth, R., Hanner, M. S., Horanyi, M., Kissel, J., Lindblad, B.-A., Linkert, D., Linkert, G., Mann, I., McDonnell, J. A. M., Morfill, G. E., Phillips, J. L., Polanskey, C., Schwehm, G., Siddique, N., Staubach, P., Svestka, J. and Taylor, A., Discovery of jovian dust streams and interstellar grains by the *Ulysses* spacecraft. *Nature* **362**, 428–430, 1993.
- Grün, E., Gustafson, B., Mann, I., Baguhl, M., Morfill, G. E., Staubach, P., Taylor, A. and Zook, H. A., Interstellar dust in the heliosphere. *Astron. Astrophys.* **286**, 915–924, 1994.
- Grün, E., Baguhl, M., Hamilton, D. P., Kissel, J., Linkert, D., Linkert, G. and Riemann, R., Reduction of *Galileo* and *Ulysses* dust data. *Planet. Space Sci.* **43**, 941–951, 1995a.
- Grün, E., Baguhl, M., Divine, N., Fechtig, H., Hamilton, D. P., Hanner, M. S., Kissel, J., Lindblad, B.-A., Linkert, D., Linkert, G., Mann, I., McDonnell, J. A. M., Morfill, G. E., Polanskey, C., Riemann, R., Schwehm, G., Siddique, N., Staubach, P. and Zook, H. A., Three years of *Galileo* dust data. *Planet. Space Sci.* **43**, 953–969, 1995b.
- Hamilton, D. P. and Burns, J. A., Orbital stability zones about asteroids II. The destabilizing effects of eccentric orbits and of solar radiation. *Icarus* **96**, 43–64, 1992.
- Hamilton, D. P. and Burns, J. A., Ejection of dust from Jupiter's gossamer ring. *Nature* **364**, 695–699, 1993.
- Horanyi, M., Grün, E. and Morfill, G. E., The dust skirt of Jupiter: a possible explanation of the *Ulysses* dust events. *Nature* **363**, 144–146, 1993a.
- Horanyi, M., Grün, E. and Morfill, G. E., The dusty ballerina skirt of Jupiter. *J. geophys. Res.* **98**, 21245–21251, 1993b.
- Humes, D. H., Results of *Pioneer* 10 and 11 meteoroid experiments: interplanetary and near-Saturn. *J. geophys. Res.* **85**, 5841–5852, 1980.
- Mann, I. and Grün, E., Dust impacts beyond the asteroid belt—a study based on recent results of the *Ulysses* dust experiment. *Planet. Space Sci.* 1993.
- Mann, I., Grün, E., Baguhl, M., Fechtig, H., Hanner, M. S., Kissel, J., Lindblad, B.-A., Linkert, D., McDonnell, J. A. M., Morfill, G. E., Polanskey, C., Riemann, R., Schwehm, G., Siddique, N. and Zook, H. A., Measurements with the *Ulysses* and *Galileo* dust detectors close to the ecliptic. *Proceedings of the 30th Liege International Astrophysical Colloquium "Observations and Physical Properties of Small Solar System Bodies"*, June 1992, Univ. de Liege, Institut d'Astrophysique, pp. 13–17, 1992.
- Riemann, R. and Grün, E., Meteor streams, asteroids and comets near the orbits of *Galileo* and *Ulysses*. *Proceeding of the Workshop on Hypervelocity Impacts in Space* (edited by J. A. M. McDonnell), pp. 120–125. University of Kent at Canterbury, 1992.
- Stone, R. G., Bougeret, J. L., Caldwell, J., Canu, P., de Conchy, Y., Cornilleau-Wehrlin, N., Desch, M. D., Fainberg, J., Goetz,

K., Goldstein, M. L., Harvey, C. C., Hoang, S., Howard, R., Kaiser, M. L., Kellogg, P., Klein, B., Knoll, R., Lecacheux, A., Langyel-Frey, D., MacDowall, R. J., Manning, R., Meetre, C. A., Meyer, A., Monge, N., Monson, S., Nicol, G., Reiner, M. J., Steinbert, J. L., Torres, E., de Villedary, C., Wouters, F.

and Zarka, P., The unified radio and plasma wave investigation. *Astron. Astrophys. Suppl. Ser.* **92**, 291–316, 1992.
Wenzel, K. P., Marsden, R. G., Page, D. E. and Smith, E. J., The *Ulysses* mission. *Astron. Astrophys. Suppl. Ser.* **92**, 207–219, 1992.